MOLECULAR AND CELLULAR BIOLOGY, Oct. 2003, p. 7163–7176 Vol. 23, No. 20
0270-7306/03/$08.00+0 DOI: 10.1128/MCB.23.20.7163–7176.2003

Steroid Receptor RNA Activator Stimulates Proliferation as Well as Apoptosis In Vivo

Rainer B. Lanz,[1]* Steven S. Chua,[1] Niall Barron,[2] Bettina M. Söder,[1] Francesco DeMayo,[1] and Bert W. O'Malley[1]

Department of Molecular and Cellular Biology, Baylor College of Medicine, Houston, Texas 77030,[1] and National Cell and Tissue Culture Center, Dublin City University, Glasnevin, Dublin 9, Ireland[2]

Received 3 March 2003/Returned for modification 8 May 2003/Accepted 7 July 2003

Steroid receptor RNA activator (SRA) is an RNA that coactivates steroid hormone receptor-mediated transcription in vitro. Its expression is strongly up-regulated in many human tumors of the breast, uterus, and ovary, suggesting a potential role in pathogenesis. To assess SRA function in vivo, a transgenic-mouse model was generated to enable robust human SRA expression by using the transcriptional activity of the mouse mammary tumor virus long terminal repeat. Transgenic SRA was expressed in the nuclei of luminal epithelial cells of the mammary gland and tissues of the male accessory sex glands. Distinctive evidence for SRA function in vivo was obtained from the elevated levels of estrogen-controlled expression of progesterone receptor in transgenic mammary glands. Although overexpression of SRA showed strong promoting activities on cellular proliferation and differentiation, no alterations progressed to malignancy. Epithelial hyperplasia was accompanied by increased apoptosis, and preneoplastic lesions were cleared by focal degenerative transformations. In bitransgenic mice, SRA also antagonized ras-induced tumor formation. This work indicates that although coactivation of steroid-dependent transcription by SRA is accompanied by a proliferative response, overexpression is not in itself sufficient to induce turmorigenesis. Our results underline an intricate relationship between the different physiological roles of steroid receptors in conjunction with the RNA activator in the regulation of development, tissue homeostasis, and reproduction.

Cancer is still a major cause of morbidity in humans due to the limited arsenal of therapies available. This lack of treatment options reflects a dearth in both general and specific scientific knowledge of tumorigenesis that exists largely because we still have not identified all the key molecular players responsible for controlled gene expression.

We have previously reported the isolation and functional characterization of a novel transcriptional coactivator, steroid receptor RNA activator (SRA) (18). SRA acts as an RNA transcript by regulating eukaryotic gene expression mediated by the steroid receptors (SRs), which play critical roles in eukaryotic development, metabolism, reproduction, and disease (23, 45). In mammalian tissue culture cells, recombinant SRA showed potent coactivation activity with the receptors for androgens (AR), estrogens (ER), glucocorticoids, and progestins (PR). However, no evidence has yet been obtained for a direct binding of SRA to SRs. We found SRA in a protein complex together with SRC coactivators and therefore proposed that SRA-containing ribonucleoprotein complexes accentuate transcriptional specificity by integrating coregulator activities upon selective binding to SRs (18). Endorsing this model, SRA was shown to associate with the DEAD box proteins p72/p68 to act as an ERα-specific ribonucleoprotein coactivator complex, which stimulates the amino-terminal activation domain of the receptor while concurrently integrating SRC/p160-mediated AF2 coactivator functions (46). Similarly, SRA was shown to bind to SHARP to modulate ER transactivation by attenuating the steroid response through sequestration while simultaneously initiating repression by SMRT (35). An analogous mechanism of transcriptional control has also been suggested for RTA (for "repressor of tamoxifen transcriptional activity"), a negative coregulator for ER (28). We have recently shown that a set of discrete stem-loop structures within SRA are required for its coactivation function and, as a result, have provided a framework on which the identification of SRA ligands and the construction of a coherent molecular model for SRA function can proceed (19).

While increasing amounts of information regarding the structure and molecular function of SRA are emerging, little is known about the physiological roles of this coactivator. SRA expression was found to be increased and aberrant in certain tumor cell lines (18) and in human breast tumors (20). To further investigate the expression profile of SRA, we first established its expression pattern in normal human tissues and then extended the analysis to human tumors. Here, we provide further evidence that SRA is significantly up-regulated in many human tumors of steroid-responsive tissues. To assess the tumorigenic potential of SRA in vivo, we generated a mouse model that uses the mouse mammary tumor virus (MMTV) long terminal repeat (LTR) to direct the expression of human SRA to the mammary glands. Because the basic aspects of murine mammary development and pathology are similar to those in the human breast (4, 29), the MMTV-transgenic tumor model has become one of the best experimental systems for evaluating the transforming and tumorigenic potential of oncogenes in vivo (reviewed in reference 15).

The MMTV LTR is expressed in a number of different cell types and tissues when inherited through the germ line (5), but it predominantly directs transgene expression to mammary

* Corresponding author. Mailing address: Department of Molecular and Cellular Biology, Baylor College of Medicine, One Baylor Plaza, Houston, TX 77030. Phone: (713) 798-6478. Fax: (713) 790-1275. E-mail: rlanz@bcm.tmc.edu.

epithelial cells (38, 42). Mammary gland development is critically sensitive to steroidal hormones. Targeted gene deletion analyses have disclosed the key physiological roles of estrogen and progesterone and their cognate receptors in mammary gland development (reviewed in reference 9 and 40). As a result, the steroid response elements in the MMTV promoter allow increased transcriptional activity at the onset of puberty, when the gland responds to systemic estrogen and growth factors with proliferation, and during pregnancy, when reproductive hormones induce the proliferation and terminal differentiation of the mammary epithelium into milk-secreting lobulo-alveoli. On abolition of the suckling stimulus, the lobulo-alveolar system undergoes involution, which is a reductive remodeling process involving extensive apoptosis and protease activity. This discontinuous development of the mammary epithelial cells as the result of exposure to endocrine hormones predisposes the tissue to aberrant proliferation, which we aimed to study with respect to SRA overexpression.

Here, we report the successful generation and analysis of transgenic mice that express human SRA under the steroid-sensitive control of the MMTV promoter in the mammary gland and tissues of the male accessory sex glands and testes. Our results show that although abundant SRA enhanced cellular proliferation and differentiation, it also promoted apoptosis and degenerative cellular functions. Overall, the data are consistent with models describing key physiological roles of SRs in development and tissue homeostasis but also suggest the existence of innate cellular survival pathways that also involve SRA-enhanced, SR-mediated control of transcription.

MATERIALS AND METHODS

Transgene construct and animals. The MMTV-SRA construct was generated by inserting a 1,262-bp fragment of the human SRA isoform II cDNA clone C10 into the *Eco*RI restriction site of the Mmtv-Sv40-BssK plasmid, which was obtained from William J. Mueller (McMaster University, Ontario, Canada). Human SRA isoform II was selected over other isolated isoforms because its extended cDNA portion 3′ of the SRA core facilitates its distinction from endogenous murine SRA, which lacks this sequence (18). The SRA cDNA includes the "core" sequence (18), the endogenous polyadenylation signal, and additional 3′ sequence but does not contain a translation initiation sequence for its extended open reading frame. The MMTV LTR control sequence originated from pA9 (14), and this vector was described previously (12). The resulting plasmid, 128-A6, was partially sequenced and tested in tissue culture settings for hormone-dependent expression of SRA. A *Xho*I-*Spe*I portion of 128-A6 devoid of vector sequences was gel purified and microinjected into stud male fertilized one-cell sFVB embryos (Harlan), which were then transferred into pseudopregnant FVB recipient females (Harlan) to carry the embryos to term. MMTV/v-Ha-ras transgenic mice, originally described as line TG.SH (38) and subsequently backcrossed into the FVB/N background (44), were obtained from Charles River Laboratory (Wilmington, Mass.). The mice were maintained under temperature-controlled (22°C), pathogen-free conditions with a 12-h light-dark cycle and fed standard rodent chow (Purina Mills Inc., St. Louis, Mo.) and fresh water ad libitum. All studies were performed under National Institutes of Health NIH guidelines for the care and treatment of experimental laboratory rodents, and applied procedures were approved for R.B.L. by the Institutional Animal Care and Use Committee of Baylor College of Medicine.

Genomic analysis and transgene expression assays. (i) DNA. Genomic DNA was purified from mouse tail tissue by digestion at 55°C overnight in 10 mM Tris-HCl (pH 7.8)–75 mM NaCl–25 mM EDTA–1% sodium dodecyl sulfate–0.25 mg of proteinase K (Roche Diagnostics, Indianapolis, Ind.) per ml followed by organic extraction and ethanol precipitation. Genotyping was routinely performed by PCR using 0.5 to 1.0 μg of genomic DNA, 10 mM deoxynucleoside triphosphate mix, 3 mM $MgCl_2$, 0.5 U of *Taq* polymerase (Promega Corp., Madison, Wis.), and 1× buffer, and the following primers: SRA (5′- CGCGGC TGGAACGACCCGCCGC and 5′-GCCAATGAAGAGAAATCTGCAGCC ACA) and ras (5′-TCGGTCCCCAGCTCTGAA and 5′-AAACACGTCTCCC CATCAATG). Endogenous mouse β-casein was targeted as PCR control with the primers 5′-GATGTGCTCCAGGCTAAAGTT and 5′-AGAAACGGAATG TTGTGGAGT. Standard PCR conditions were 30 cycles of denaturation for 1 min at 94°C, primer annealing for 45 s at 60°C, and synthesis for 30 s at 72°C. For Southern analysis, genomic DNA was digested with *Eco*RI and *Bam*HI and blotted as described previously (8). Transgene copy numbers were determined by quantitative real-time PCR (qPCR [see below]) against a serial dilution of pSCT-SRA2 plasmid (18) as reference standard.

(ii) RNA. Total RNA from human and animal tissues was isolated as described previously (6), separated by formaldehyde-agarose gel electrophoresis, and transferred by capillary force to a Zetaprobe GT membrane (Bio-Rad Laboratories Inc., Hercules, Calif.). The UV-immobilized RNA was analyzed with the following probes, which were generated using a random DNA-labeling kit (Life Technologies) and 50 μCi of [α-^{32}P]dCTP, (300 Ci/mmol [ICN]) followed by G-50 (Roche) column purification: a 1.3-kb probe corresponding to SRA C10 was used to detect human SRA on the MTE array (Clontech Laboratories Inc. Palo Alto, Calif.), the Northern Territory-Human Tumor Panel Blot IV (Invitrogen Co. Carlsbad, Calif.), and the primary human tissue blots; a probe against the *Ase*I-*Spe*I fragment of the transgene construct containing the 3′ portion of SRA and the simian virus 40 (SV40) polyadenylation sequence from the vector detected SRA in transgenic RNA; a probe against clone 83-H10 (AF092039 [18]) was specific for endogenous mouse SRA; and an 18S probe (Invitrogen) was used as an internal control. Isolated RNA used for qPCR analysis was treated with RNase-free DNase (Roche) and subsequently column purified with RNeasy (Qiagen, Valencia, Calif.).

qPCR. About 200 ng of total RNA was reverse transcribed with random hexamer primers and the murine leukemia virus reverse transcriptase GeneAmp RNA PCR kit (PE Applied Biosystems, Foster City, Calif.) for 40 min at 48°C in a 100-μl reaction volume. Then 2 μl (0.027 μl) of reverse transcription RT product was analyzed for human SRA and 18S RNA expression by real-time PCR using the TaqMan Universal PCR chemistry (Applied Biosystems) on the ABI Prism PE7700 sequence analyzer (Applied Biosystems). Gene-specific primers and probes were designed using Primer Express software (Applied Biosystems) and following the guidelines provided by Applied Biosystems. The amplicon for SRA was 74 bp long, extended over exons 4 and 5 of *sra*, and consisted of the primers 5′ TGGCTCTACTGGTGCAAGAGC (T_m = 59°C) and 5′ AA CCATGAGGGAGCGGTG (T_m = 58°C) and the 5′-6FAM- and 3′-TAMRA-conjugated probe 5′-CATCTGCTGCGTCCCACCGGT (T_m = 68°C). The amplicon for Ras used the primers 5′ CTGACCATCCAGCTGATCCAG (T_m = 59°C) and 5′ ACACGTCTCCCCATCAATGAC (T_m = 58°C), and the probe 5′-FAM-ATCCCACTATAGAGGACTCCTACCGGAAACAGG-TMARA (T_m = 69°C). We used 600 nM primers and 200 nM probe in 50-μl reaction volumes in MicroAmp 96-well plates. The thermal cycling conditions were AmpErase UNG activity for 2 min at 50°C, AmpliTaq Gold DNA polymerase activation for 10 min at 95°C, and 40 cycles of 15 s at 95°C and 1 min at 60°C. Cycle threshold values (Ct) were analyzed using SDS1.9 software (Applied Biosystems). Singleplex SRA quantities were normalized against 18S RNA amplification (primer-probe set from Applied Biosystems), for which input cDNA was diluted 75-fold. Relative expression levels were determined by the comparative Ct method (*ABI Prism 7700 SDS User Bulletin no. 2;* Applied Biosystems). The slope of log input amount versus δCt was −0.01, indicating similar amplification efficiencies of SRA and the 18S RNA reference.

Serum analysis and hormone treatment. Serum analyses (testosterone, progesterone, and growth hormone [GH]) were carried out with DSL-RIA kits (Diagnostic Systems Laboratories, Inc., Webster, Tex.) as specified by the manufacturer. To mimic pregnancy, beeswax pellets containing approximately 20 mg of progesterone and 20 μg of estradiol (provided by John Lydon, Baylor College of Medicine) were implanted subcutaneously and replaced after 2 weeks. Mammary glands were analyzed after hormone stimulation for a total of 4 weeks.

In situ hybridization. Standard in situ hybridization methods for paraffin-embedded tissue were used (10, 24). Antisense and control sense riboprobes were synthesized on *Xho*I- and *Xba*I-linearized plasmid templates, respectively, containing the 611-bp *Hin*cII-*Eco*RI cDNA fragment of SRA. The purified cDNA fragments were labeled with 0.25 mM each GTP, ATP, and CTP together with 100 mCi of [^{35}S]UTP (Amersham Pharmacia Biotech, Piscataway, N.J.) and T7 or T3 (for the antisense and sense riboprobe, respectively) RNA polymerase (Promega) at 37°C for 2 h. DNase-treated probes were purified by organic extraction and G-50 gel filtration (Roche) and yielded 1×10^6 to 2×10^6 cpm/μl. A probe concentration of 2.5×10^6 cpm was used on each tissue slide. Following autoradiography on BioMax MR film (Kodak, Rochester, N.Y.), the slides were dipped in NTB-2 emulsion (Kodak) for 1 to 2 days in a light-tight box, developed, fixed, counterstained in hematoxylin, and coverslipped for analysis.

Whole mounts and histology. The inguinal (abdominal) mammary glands at various stages of development were dissected, mounted on glass slides, and fixed for 4 to 8 h in Carnoy's fixative (60% ethanol, 30% chloroform, 10% glacial acetic acid). The tissues were washed in 70% ethanol, gradually hydrated in distilled water, and stained in carmine alumn (C1022 and aluminum potassium sulfate [A7167; Sigma, St. Louis, Mo.]) overnight at 4°C. Mammary glands then were dehydrated by subsequent 15-min washes in 70, 90, and 100% ethanol, cleared in xylene, and stored in methyl salicylate (Sigma M6752). Whole mounts were analyzed under a STEMI 2000 CS microscope (Carl Zeiss, Jena, Germany) and pictured with a Coolpix 990 digital camera (Nikon Inc., Tokyo, Japan). Tissues for histology were fixed in buffered formalin (pH 7.2) (mammary glands and salivary glands), 2% paraformaldehyde (pH 7.4) (prostate, seminal vesicle [SV], vas deferens, ampulla, bulbourethral gland, and preputial gland), Bouin's fixative (testis and epididymis), or 2% paraformaldehyde–0.2% glutaraldehyde–0.02% NP-40–phosphate-buffered saline (pH 7.4) (testis and epididymis used for immunohistochemistry) overnight at 4°C, washed in phosphate-buffered saline, and gradually dehydrated and stored in 70% ethanol until used for paraffin embedding. Tissue sections (5 μm thick) mounted on glass slides were processed and stained with hematoxylin and eosin (H&E) or periodic acid-Schiff by standard methods. For proliferation studies, the mice were given an intraperitoneal injection of 5-bromo-2-deoxyuridine (BrdU; Amersham Pharmacia Biotech, Piscataway, N.J.) at a dose of 100 μg/g of body weight 2 to 7 h prior to sacrifice. For immunohistochemistry, monoclonal BrdU antibody (Zymed, South San Francisco, Calif.), a rabbit anti-human PR polyclonal antibody (DAKO, Carpinteria, Calif.), mouse mononuclear phagocyte-specific Mac-3 monoclonal antibody (Pharmingen-BD Biosciences, San Diego, Calif.), mouse monoclonal antibodies AR 441 (Santa Cruz Biotechnology Inc, Santa Cruz, Calif.) and AR-318 (Novocastra, Newcastle, United Kingdom) against androgen receptor were used in protocols provided by the manufacturer of the antibodies or as previously published (30, 31, 34). Histological testing was performed with an Axioplan 2 microscope and Plan-Neofluar objectives (Zeiss), and images were captured with a Focus HR2C HR digital color camera system (Focus, Houston, Tex.), processed with Adobe Photoshop 7.01 and Illustrator 10.02 (Adobe Systems Inc., San Jose, Calif.), and archived using AppleScript- and FileMaker (Apple Inc., Cupertino, Calif.)-based software solutions developed by RBL.

Tissue culture and transient-transfection assay. Human cervical carcinoma (HeLa) cells were routinely maintained in Dulbecco modified Eagle medium plus 10% fetal bovine serum. At 24 h before transfection, 3×10^5 cells per well of a six-well plate or 10^5 cells per 12-well dish were plated in Dulbecco modified Eagle medium containing 5% dextran-coated charcoal-stripped fetal bovine serum. The cells were transfected with Superfect transfection reagent (Qiagen) as specified by the manufacturer. Transfection assay was described previously (18).

RESULTS

SRA is overexpressed in human tumors of steroid-responsive tissues. To assess the pattern of SRA expression in normal human tissues, we first hybridized an MTE array with SRA-specific probes. Table 1 illustrates a subset of the results. Based on this normalized blot, and relative to the average SRA expression levels of all human tissues on the blot, SRA was highly expressed in the adrenal gland, pituitary gland, and liver but was expressed at low levels in the breast, ovary, uterus, and prostate. The lower abundance of SRA in normal steroid-responsive tissues is remarkable when considering the selective function of SRA for steroid receptors.

The analysis of a commercial human tumor panel blot, however, indicated that SRA was significantly up-regulated in tumors of the breast, uterus, and ovary but was not overexpressed in a tumor of the fallopian tube (Fig. 1A). Similar results were obtained with primary tissue samples; compared to normal tissue, SRA was up-regulated in 12 of 13 ovarian tumor samples tested and in all available uterine tissues that pathologists had identified as tumors (Fig. 1B). Northern analysis of human breast tissues disclosed a similar pattern by showing that SRA was up-regulated in 90% of the tumor samples tested ($n = 36$). To assess the amplitude of SRA expression in these tumor samples, we also performed qPCR analysis using SRA- and 18S endogenous control RNA-specific sequences (Fig. 1C). While normal breast tissue ($n = 7$) showed the expected low SRA-to-18S ratios, SRA transcripts were found to be approximately sixfold up-regulated in tumors of the breast ($n = 29$). When the results were grouped according to tumor type, quantitative expression analysis showed that the mean relative SRA levels were similarly augmented in infiltrating ductal tumors, breast fibroadenomas, and another group consisting of mostly high-grade breast adenocarcinomas and infiltrating carcinomas (Fig. 1C). These results indicated that SRA overexpression may correlate with proliferation but does not correlate with tumor type or grade. A different frequency of SRA up-regulation was found in other human tumors tested; Northern analysis indicated that SRA was up-regulated in only two of nine tumors of the pancreas and in three of nine kidney tumors (not shown), suggesting that the up-regulation of SRA was specific for transformed steroid-dependent tissues and did not reflect tissue heterogeneity or epithelial cell content. We concluded that SRA is significantly up-regulated in human tumors of the breast, ovary, and uterus and next assessed its oncogenic potential in vivo.

TABLE 1. SRA expression in normal human tissues[a]

Tissues (MTE array)	Relative SRA expression (%)
Mean all tissues	100
Brain[b]	90
Pituitary gland	225
Heart[b]	104
Lungs	132
Gastrointestinal tract[b]	95
Skeletal muscle	140
Liver	224
Kidneys	124
Adrenal gland	343
Breasts	50
Ovaries	41
Uterus	57
Prostate	76
Testes	162

[a] Selected data from a comprehensive Northern analysis based on an MTE array (Clontech) probed for human SRA expression are shown. The membrane carries normalized quantities of poly(A)$^+$ RNA from 76 different human tissues and different control RNAs and DNAs. Values indicate SRA transcript levels relative to the mean SRA expression of all tissues on the blot, as determined by PhosphorImager evaluation and three different densitometer readings of two separate hybridization events.

[b] Mean of multiple subtissues.

Generation and characterization of MMTV SRA-transgenic mouse lines. To study SRA function in vivo and to determine whether overexpression of SRA alone is sufficient to initiate tumor formation, we generated a mouse model that uses the MMTV LTR to direct the expression of human SRA to the murine mammary glands. Two separate microinjections of linearized transgenic cDNA construct devoid of vector sequences (Fig. 2A) into mouse zygotes from an inbred FVB colony produced five founder mice whose progeny inherited SRA in a Mendelian fashion.

We first analyzed each of the transgenic lines for the expression of SRA in the mammary glands. Northern analysis of mammary tissues from 4- to 6-month-old virgin animals of the

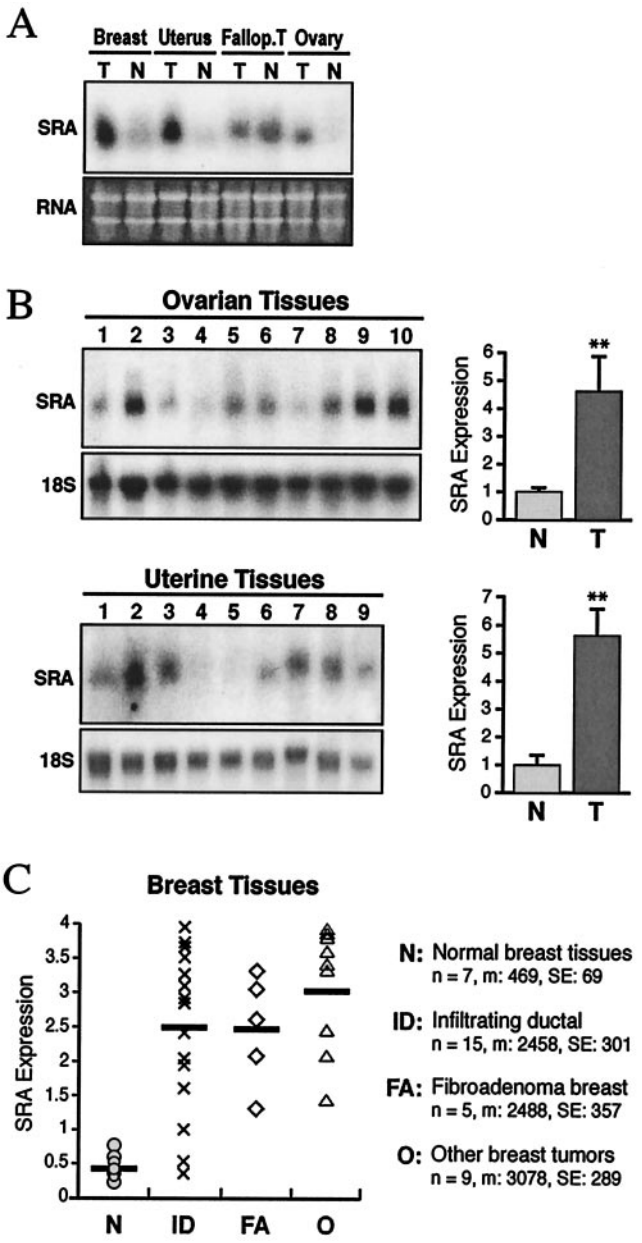

FIG. 1. SRA is up-regulated in human steroid-dependent tumors. (A) Northern Territory-Human Tumor Panel Blot IV (Invitrogen) hybridized with a radioactively labeled cDNA probe for human SRA (SRA) and visualization of an ethidium bromide (EtBr)-stained gel after electrophoresis (RNA). The blot represents 20 μg of total RNA isolated from four different human tumor (T) and normal (N) tissues. (Breast) Invasive ductal carcinoma of breast and normal breast tissue from a female aged 51. (Uterus) Well-differentiated adenocarcinoma of endometrium and normal uterine tissue from a female aged 55. (Fallop.T) Adenocarcinoma of fallopian tube and normal fallopian tube from a female aged 46. (Ovary) Mucinous cystandenocarcinoma of ovary and normal ovarian tissue from a female aged 67. (B) Northern analysis of *SRA* gene expression in human ovarian and uterine tissues. About 20 μg of total RNA isolated from different local donor's ovarian (top) and uterine (bottom) tissues was separated on a 1.4% denaturing agarose–formaldehyde gel, blotted onto a nitrocellulose membrane and hybridized with a labeled cDNA probe for human SRA (SRA) and control 18S rRNA (18S). The mean relative expression levels of SRA in normal (N) and tumor (T) tissues based on densitometric readings of different film exposures of the blots are shown to the right. (Ovarian Tissues) Lanes 1, 3, and 5, adenocarcinoma of the ovary from females aged 59, 38, and 42, respectively; lanes 2 and 10, papillary serous carcinoma of the ovary from females aged 51 and 57, respectively; lane 4, normal uterine tissue, from a female aged 68; lane 6, Endometrioid adenocarcinoma of the ovary from a female aged 65; lane 7, Sertoli cell tumor from a female aged 31; lanes 8 and 9, Mucinous cystadenona of the ovary from females aged 87 and 31, respectively; **, significant differences between normal ($n = 5$) and tumor ($n = 13$) tissues (*t* test, $P = 0.000032$). (Uterine tissues) Lane 1, Endometrial tumor from a female aged 59; lane 2, leiomyoma of the uterus from a female aged 41; lane 3, adenocarcinoma of the uterus from a female aged 66; lanes 4 and 5, normal uterine tissues from females aged 66 and 55, respectively; lane 6, endometrial tissue from a female aged 51; lane 7, Endometrioid adenocarcinoma of the uterus from a female aged 59; lane 8, moderately differentiated adenocarcinoma of the uterus from a female aged 65; lane 9, well-differentiated adenocarcinoma of the uterus from a female aged 65; **, significant differences between normal ($n = 2$) and tumor ($n = 7$) tissues (*t* test, $P = 0.00087$). (C) qPCR analysis of SRA expression in human breast tissues. Total RNA isolated from 36 pathologically characterized breast samples obtained from a local breast tumor tissue bank was reverse transcribed and subsequently analyzed for SRA and 18S control RNA expression. Singleplex SRA quantities were normalized against 18S RNA amplification. Relative SRA expression levels were determined by the comparative Ct method (see Materials and Methods) and are presented for the tissues pathologically grouped as normal breast tissues (N), infiltrating ductal (ID), breast fibroadenomas (FA) and other breast tumors (O, consisting of adenocarcinomas, apocrine metaplasia, metaplastic carcinoma and juvenile hypertrophy). Number of specimens (n), mean expression levels (m), and standard error (SE) are indicated for each group. The mean SRA expression level of the combined breast tumor tissues is 2,656 (*t* test, $P < 0.00001$).

first filial generation (F_1) indicated genotype-specific SRA expression, which was very strong for progenies of the 6413 founder and was moderate in the other lines (Fig. 2B). When the same RNA preparation was examined for endogenous SRA expression, Northern analysis showed that transgenic human SRA was expressed at higher levels than was endogenous murine SRA and that the auxiliary expression of the ortholog had little effect on the endogenous levels of mouse SRA (Fig. 2B), suggesting that SRA expression is unlikely to be controlled by an autoregulatory mechanism. We then used qPCR to evaluate the transgene copy number in animals from the second filial generation (F_2). The transgenic founder 6413 did not produce viable offspring beyond the F_1 generation, and of the remaining four transgenic lines, only progeny of the founder stud 6411 had multiple copies of SRA integrated into the genome (Fig. 2C). Also, this line segregated SRA in Mendelian conformity, indicating that multiple copies of the transgene had integrated into a single chromosome. With respect to transgene expression, this line was similar to the other three remaining founder lines, although it produced offspring that showed poorer fertility in transgenic males than did to progeny from other lines possessing single transgene integration (below).

We next determined the tissue specificity of transgene expression and used Northern blotting and qPCR to analyze total RNA extracted from various murine tissues of transgenic F_2 mice derived from 6411 and 6612 founder lines (Fig. 2D). Apart from the high levels of transgene expression present in the female mammary glands, moderate levels of SRA were also detected in the salivary gland and trace levels of SRA were identified by qPCR in lung and uterine tissue (Fig. 2D). Con-

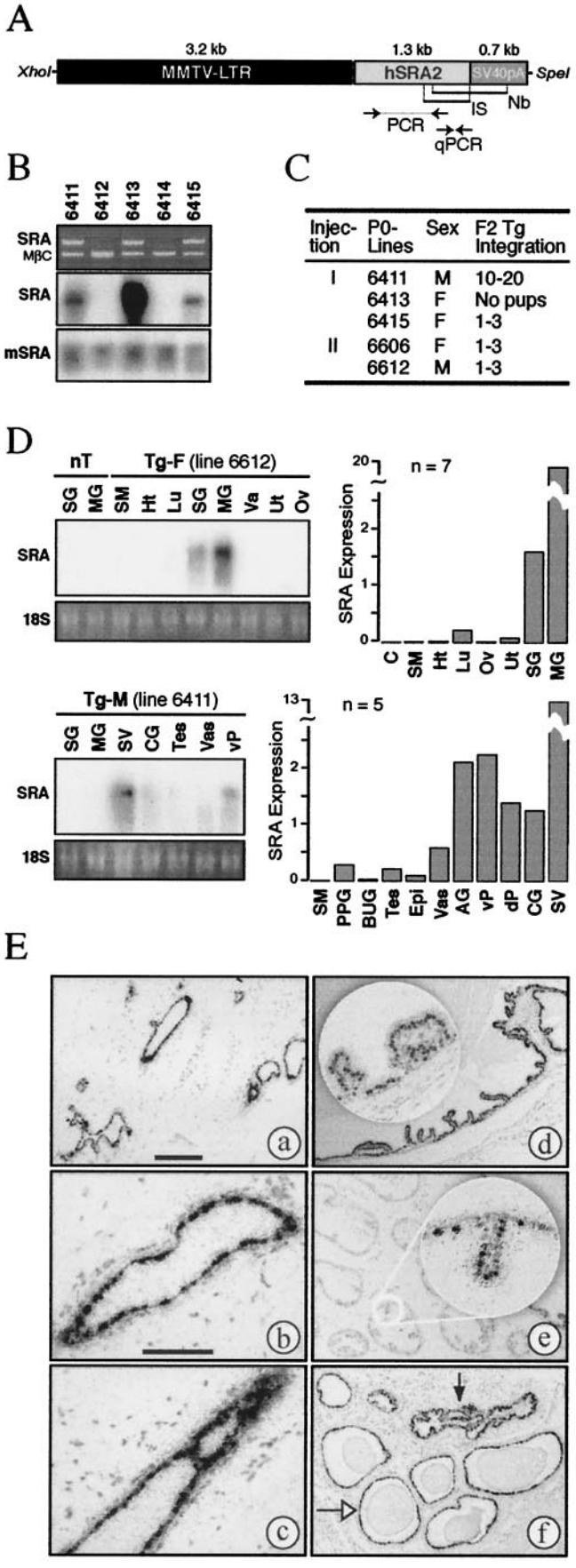

sistent with the tissue-specific pattern of transgene expression seen in other MMTV-driven transgenic strains (7, 38, 42), human SRA was also detected in the organs of the male urogenital system. Relatively strong transgene expression was discovered in the SVs and lower SRA levels were found in the ampullary gland and in all lobes of the prostate, of which the ventral prostate consistently showed the highest levels of SRA expression. Transgene expression in the vas deferens, testis, and prepuital gland was minimal and only detected by qPCR.

FIG. 2. Generation and characterization of SRA-transgenic mice. (A) Transgenic construct. The construct used for the generation of SRA-transgenic mice consists of the hormone-responsive MMTV LTR promoter-enhancer controlling human SRA isoform II and an additional SV40 polyadenylation signal (SV40pA). A 5.2-kb *Xho*I-*Spe*I fragment devoid of vector sequences was microinjected into mice oocytes. Sequences used for the characterization of transgenic animals are indicated as follows: Nb, cDNA probe for Northern blot analysis; IS, riboprobe for in situ expression analysis; PCR, primer pair for PCR-based genotyping; qPCR, amplicon used for qPCR analysis. (B) Genomic characterization of SRA-transgenic animals. Representative mouse gDNA analysis by PCR followed by EtBr-agarose gel analysis for SRA-transgene (SRA) integration and endogenous mouse β-casein (MβC; BC003863) control reference (top), and Northern analysis for transgene (SRA, center) and endogenous mouse SRA (mSRA, bottom) expression from mammary gland tissues of 4- to 6-month old virgin F_1 female animals. 6411, 6413, and 6415 indicate SRA-transgenic founder animals, 6412 and 6414 are nontransgenic mice. SRA-specific PCR primers and probes used for the analyses are indicated in panel A; mouse cDNA clone H10 (18) was used to generate the mSRA-specific radioactively labeled probe. (C) SRA-transgenic founder lines and transgene integration. Transgenic F_2 pups from four different SRA-transgenic founder mice (P0, derived from two separate injections I and II) were analyzed by qPCR for SRA transgene integration. Potential founder line 6413 did not produce viable pups. Approximate transgene copy numbers were standardized against SRA cDNA plasmid amplification. M, male; F, female. (D) Transgene expression analysis. Northern analysis for human SRA-transgene expression (SRA) and UV visualization of EtBr-agarose gel for RNA input control (18S) of selected tissues from nontransgenic (nT) and SRA-transgenic multiparous female littermates (Tg-F, top) or age-matched (8.2-month-old) transgenic male (Tg-M, bottom) from the indicated founder lines are shown on the left. The graphs to the right show qPCR analyses of pooled RNA samples from two nontransgenic mammary glands (C) and different tissues from seven transgenic females (top), and from five transgenic male mice (bottom) from both lines analyzed (lines 6411 and 6612). Singleplex SRA quantities were normalized against 18S RNA amplification, and relative expression levels are shown compared to normalized amplification of liver RNA. Selected tissues from which total RNA was prepared are as follows: SG, salivary gland; MG, mammary gland; SM, skeletal muscle; Ht, heart; Li, liver; Va, vagina; Ut, uterus; Ov, ovary; Lu, lung; SV, seminal vesicle; CG, coagulating gland (anterior prostate); Tes, testis; Vas, vas (ductus) deferens; vP, ventral prostate; PPG, preputial gland; BUG, bulbourethral gland; Epi, epididymis; AG, ampullary gland; dP, dorsal prostate. (E) In situ hybridization analysis for SRA expression in selected transgenic tissues. Micrographs a to c show tissue sections from the abdominal mammary gland of mature transgenic virgins, indicating strong SRA expression in almost all mammary gland luminal epithelial cells. Micrographs d to f show relatively strong transgene expression in tissues of the male accessory sex glands: (d) SV, (e) coagulating glands, (f) ampullary gland (solid arrow) and ventral prostate (open arrow). Higher-magnification pictures as insets in panels d and e show nuclear expression of SRA in the luminal epithelial cells of the seminal vesicle and coagulating gland, respectively. Representative tissues are from sexually unchallenged adult SRA-transgenic F_2 progeny from founder lines 6612 (a, b, and e) and 6411 (c, d, and f). Bar in panel a, 250 μm (also applies to panels d to f); bar in panel b, 100 μm (also valid for panel c).

No human SRA RNA was found in liver, skeletal muscle, heart, or ovary of transgenic animals, or in any tissues from wild-type mice (Fig. 2D). This profile of transgene expression was confirmed by in situ hybridization analysis of sections derived from mature carrier animals and age-matched wild-type tissues (Fig. 2E). In addition, in situ analysis traced SRA transcripts to the nuclei of the luminal epithelial cells of the mammary ducts (Fig. 2E, micrographs a to c) and the nuclei of the epithelial cells of the male accessory sex glands (micrographs d to f), showing an almost uniform expression pattern in the mammary glands and seminal vesicles.

While there was some variation among animals with respect to transgenic SRA levels, expression in the mammary glands accompanied morphological changes in the tissue since transgene levels increased during the juvenile stages of mammary gland development, peaked at early pregnancy, decreased during lactation, and were low during involution (data not shown). This observation is in agreement with the steroid-regulated profile of the MMTV promoter. In summary, we have successfully targeted the murine mammary glands for robust SRA expression. We next assessed the phenotypic consequences of this overexpression.

Impaired fertility of SRA-transgenic mice. Throughout our analysis of progeny from all founder lines, it became evident that an important phenotype of SRA overexpression was poor breeding success. When considering all breeding pairs used over a total period of 20 months, more than half of the breeder pairs did not produce progeny, and the average litter sizes for breeder pairs from the lines 6411 and 6612 were 2.5 and 3.0 pups, respectively (Fig. 3A). In addition to poor fertility, 30 and 15% of pups of lines 6411 and 6612, respectively, died before reaching weaning age. To determine whether the breeding problems were sex dependent, only breeder pairs consisting of a transgenic and a wild-type animal were analyzed. In this case, transgenic males of both lines analyzed (6411 and 6612) produced average litter sizes of 2 and 4 pups, respectively, and were slightly less successful at generating offsprings than were transgenic females, which averaged 5.2 and 6.0 pups in lines 6411 and 6612, respectively. Because wild-type FVB breeders in our housing environment produced 10 to 12 pups on average, these numbers clearly indicate that fertility was impaired in SRA-transgenic animals of both sexes.

The analysis of mixed transgenic/wild-type breeder pairs also revealed that in both lines analyzed the survival rate of progeny from transgenic mothers and wild-type fathers was poorer than in pairs containing wild-type mothers. This observation was supported by initial growth and body weight studies, which disclosed that pups from transgenic mothers and wild-type fathers developed poorly and attained only 30 to 50% of the body weight of pups from wild-type mothers at weaning age (Fig. 3B). When newborns were given to foster mice, the pups acquired normal body weights, strongly indicating a likely defect in the transgenic mammary glands. We therefore decided to first study SRA-transgenic mammary glands for possible tumorigenic events.

Histopathology of SRA-transgenic mammary glands. To analyze for physiological perturbations caused by the overexpression of SRA, we performed whole-mount analysis and histology on the inguinal (abdominal no. 4) female mammary gland at various stages of its development.

A

	All BP				Tg x WT; 6411				Tg x WT; 6612			
	6411		6612		Tg-F		Tg-M		Tg-F		Tg-M	
	#	%	#	%	#	%	#	%	#	%	#	%
Total BP:	223	100	117	100	21	100	90	100	21	100	32	100
Unsuccessful:	121	54	59	50	6	29	55	61	4	19	14	44
Litter Size:	2.5		3.0		5.2		2.0		6.0		4.0	
Total Pups:	561	100	355	100	110	100	182	100	126	100	129	100
Tg:	264	47	178	50	28	25	78	43	54	43	60	47
WT:	297	53	177	50	82	75	104	57	72	57	69	53
† Pups *:	87	16	38	11	33	30	7	4	19	15	9	6
F-pups :	238	42	174	49	30	27	83	46	62	49	69	53
M-pups :	236	42	141	40	47	43	92	50	45	36	51	40

BP, Breeding Pairs; Tg, transgenic; WT, wild-type; 6411, 6612, SRA-transgenic lines; F, Females; M-Males; *, deceased before weaning.

B

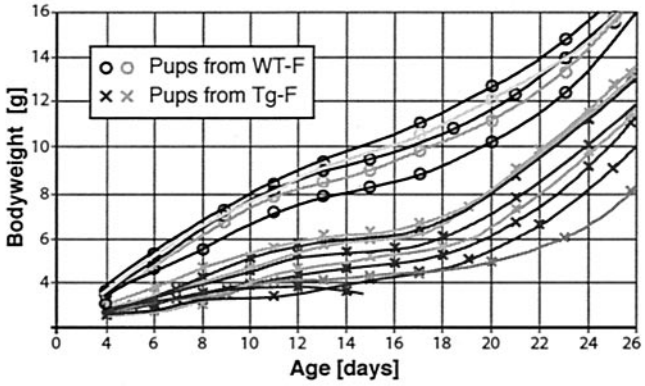

FIG. 3. Impaired fertility in SRA-transgenic mice and abnormal growth curves in pups derived from transgenic mothers. (A) The table shows breeding statistics of the entire transgenic colony (all breeding pairs [All BP]) as well as a line-dependent analysis (center and right columns apply to transgenic lines 6411 and 6612, respectively). "All BP" comprise SRA-heterogeneous (Tg × WT) as well as SRA-homogenous (Tg × Tg) breeding partners and includes repetitive breeding attempts. Unsuccessful breeders did not produce embryos during 35 days of breeding; deceased pups died before postpartum day 21. #, count of pups; %, percentage. The analysis indicated that fertility was impaired in both transgenic males and females of both lines, and SRA males derived from founder 6411 were the least successful in producing progeny. (B) The diagram illustrates early body weight development from representative progeny of both sexes and genotypes derived from SRA-transgenic mothers (crosses) or wild-type mothers (circles).

(i) Ductal ectasia and alveolar development in virgin mammary glands expressing transgenic SRA. While early ductal outgrowth in SRA-transgenic strains was comparable to gland development of wild-type FVB control mice, mature virgin carriers showed aberrant mammary gland development consisting of ductal ectasia with grossly irregular and partially convoluted gland morphology (Fig. 4b and d). In older virgin transgenic animals, the ducts were typically expanded and often contained eosinophilic proteinaceous secretions. They also displayed acinar hyperplasia, as evidenced by countless small spicules and side buds that covered the entire ductal system (Fig. 4f and h). This appearance resembled normal alveolar development during early pregnancy, which was not in agree-

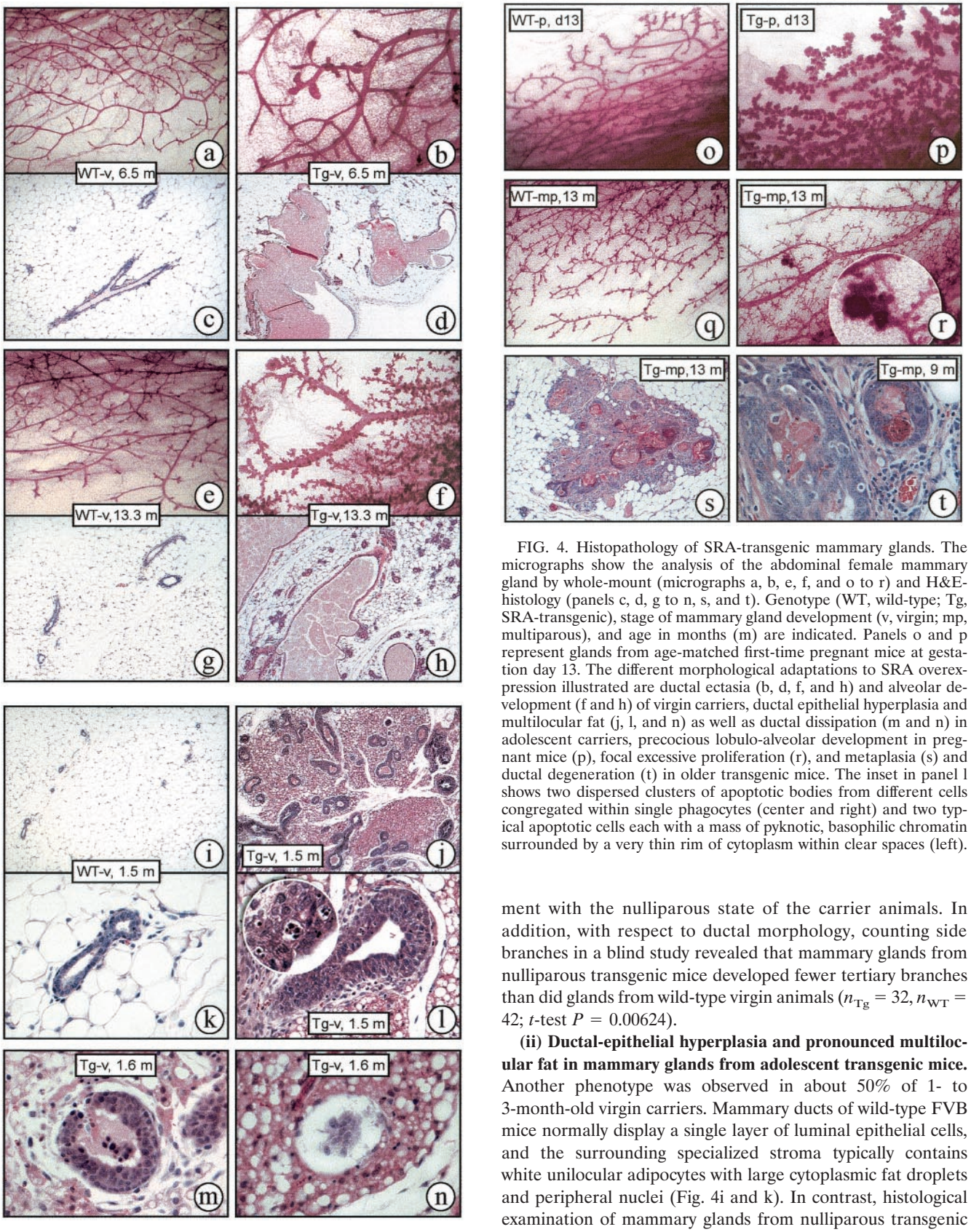

FIG. 4. Histopathology of SRA-transgenic mammary glands. The micrographs show the analysis of the abdominal female mammary gland by whole-mount (micrographs a, b, e, f, and o to r) and H&E-histology (panels c, d, g to n, s, and t). Genotype (WT, wild-type; Tg, SRA-transgenic), stage of mammary gland development (v, virgin; mp, multiparous), and age in months (m) are indicated. Panels o and p represent glands from age-matched first-time pregnant mice at gestation day 13. The different morphological adaptations to SRA overexpression illustrated are ductal ectasia (b, d, f, and h) and alveolar development (f and h) of virgin carriers, ductal epithelial hyperplasia and multilocular fat (j, l, and n) as well as ductal dissipation (m and n) in adolescent carriers, precocious lobulo-alveolar development in pregnant mice (p), focal excessive proliferation (r), and metaplasia (s) and ductal degeneration (t) in older transgenic mice. The inset in panel l shows two dispersed clusters of apoptotic bodies from different cells congregated within single phagocytes (center and right) and two typical apoptotic cells each with a mass of pyknotic, basophilic chromatin surrounded by a very thin rim of cytoplasm within clear spaces (left).

ment with the nulliparous state of the carrier animals. In addition, with respect to ductal morphology, counting side branches in a blind study revealed that mammary glands from nulliparous transgenic mice developed fewer tertiary branches than did glands from wild-type virgin animals ($n_{Tg} = 32, n_{WT} = 42$; t-test $P = 0.00624$).

(ii) Ductal-epithelial hyperplasia and pronounced multilocular fat in mammary glands from adolescent transgenic mice. Another phenotype was observed in about 50% of 1- to 3-month-old virgin carriers. Mammary ducts of wild-type FVB mice normally display a single layer of luminal epithelial cells, and the surrounding specialized stroma typically contains white unilocular adipocytes with large cytoplasmic fat droplets and peripheral nuclei (Fig. 4i and k). In contrast, histological examination of mammary glands from nulliparous transgenic mice revealed several layers of luminal epithelial cells, indicating strong intraductal proliferation, as well as multilocular adi-

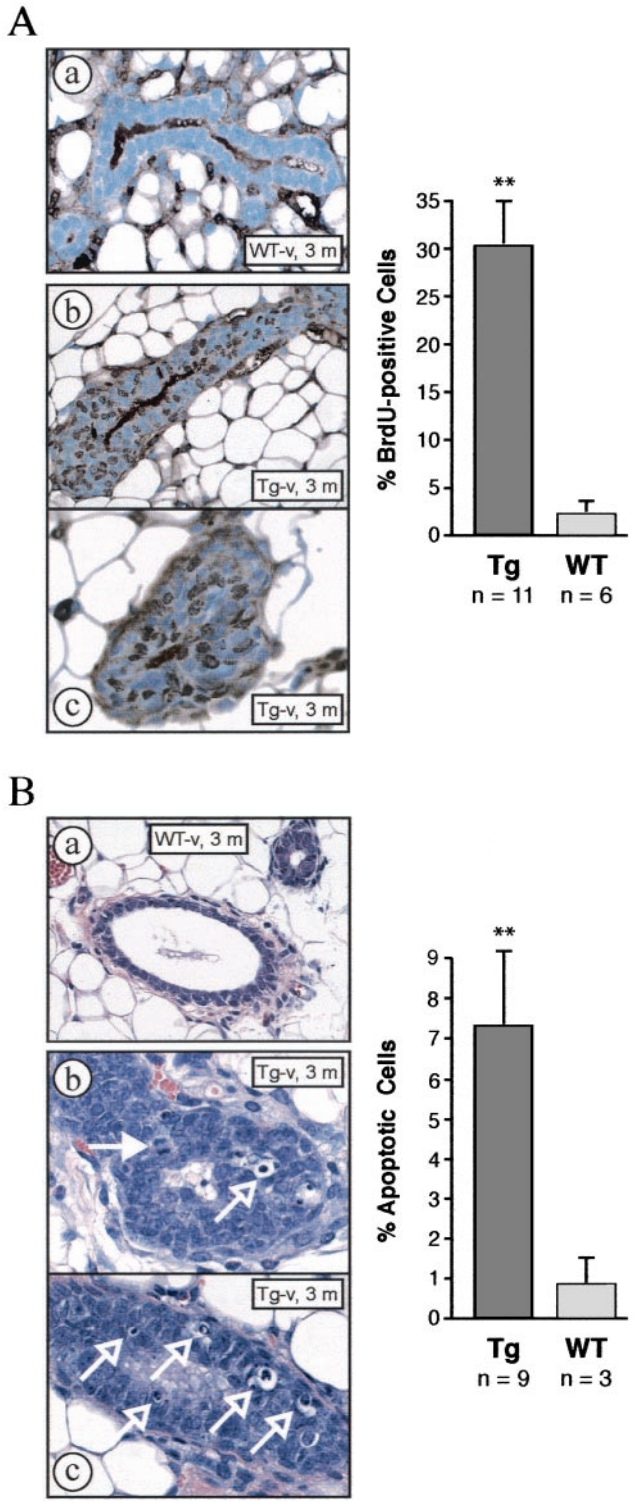

FIG. 5. Elevated proliferation and apoptosis in SRA mammary glands. (A) SRA expression increased the proliferation of mammary luminal epithelial cells. The micrographs show BrdU immunohistochemistry of mammary gland sections from age-matched wild-type (WT) (micrograph a) and transgenic (Tg) (micrographs b and c) virgin mice. The graph illustrates the percentage of total mammary gland epithelial cells positive for BrdU immunosignal. 1433 transgenic and 485 wild-type cells were counted (*t* test, $P < 0.00001$). (B) Adjacent sections of the glands that were analyzed for BrdU incorporation (A) were also examined microscopically for apoptosis. The panels show representative sections of wild-type glands (micrograph a) and transgenic glands from lines 6411 (micrograph b) and 6612 (micrograph c), illustrating multiple pyknotic phagocytes in the transgenic sections (open arrows). In panel b, dividing cells (solid arrow) and phagocytosis of apoptotic cells (open arrow) indicate concurrent mitosis and apoptosis. The graph illustrates the percentage of total mammary gland epithelial cells showing apoptosis by microscopic examination (*t* test, $P < 0.00001$).

pose tissue with cells containing a central nucleus surrounded by multiple dense fat droplets (Fig. 4j and l to n). The stratified epithelia also contained many vacuolated structures with heteromorphic content, which were identified as apoptotic bodies and fragmented epithelial cells (inset in Fig. 4l). Transgenic mammary glands showing ductal hyperplasia also displayed numerous degenerating ducts with suspicious accumulations of lymphocytes and macrophages at the dissipating structures (Fig. 4m and n). This abnormal process of ductal luminal hyperplasia and concurrent apoptosis and ductal degeneration was observed less often as the nulliparous transgenic animals aged but was typically accompanied by obvious changes in the fat pad. The high degree of plasticity of the mammary duct system and the dedifferentiation of large unilocular fat cells into smaller multiloculated adipocytes not only suggested that SRA-transgenic animals showed increased susceptibility to reproductive hormones but also hinted at a possible role of SRA in adaptive thermogenesis.

(iii) Precocious lobulo-alveolar development in pregnant SRA glands. Having established distinct phenotypic consequences of SRA overexpression in the virgin mammary gland, we next studied mammary gland morphology in pregnant animals. During pregnancy, PR mediates the systemic effects of progestins to ensure lobulo-alveolar development. Because PR is also a target for SRA coactivation, we expected significant alterations in the gland morphology of transgenic mice. We discovered precocious ductal-alveolar mammary gland development in SRA-transgenic mice as early as 1 week into gestation. Whole-mount analysis indicated that the transgenic abdominal mammary glands at gestation day 13 displayed alveolar structures comparable to the glands of wild-type animals at parturition (Fig. 4p). Given these results, we concluded that the function of PR in the genesis and progression of lobulo-alveolar structures was potentiated in SRA-transgenic animals. Interestingly, alveolar hyperplasia was moderate in nulliparous SRA animals under a systemic regimen of estrogen and progesterone (data not shown), indicating that the exogenous administration of steroids could not reproduce the full spectrum of complex hormonal changes that occurs during a normal pregnancy. During lactation, transgenic mammary glands displayed dense lobulo-alveolar structures that occupied the majority of the intraductal space of the fad pad. Extensive ductal hyperplasia as a causative factor for not nursing to the young properly has been reported before (21) and may have also played a role in the survival rate of SRA transgenic pups. Still, the morphology of the lactating mammary gland, as well as the appearance of transgenic glands during involution, grossly resembled the glandular structure of wild-type glands, and therefore was not further investigated.

(iv) Focal metaplasia and dissipating ducts in older SRA-mammary glands. We next analyzed SRA-derived phenotypic changes in multiparous animals. Repetitive parturition did not accentuate the phenotypes observed in transgenic glands. As multiparous transgenic animals aged, however, whole-mount analysis and histology revealed the sporadic appearance of small preneoplastic lesions such as the focal excessive proliferation of branching tubules (Fig. 4r and s). These lesions never progressed to authentic malignancies, but they attracted macrophages and lymphocytes and developed into focal degenerative transformations of glandular to stratified squamous epithelia (Fig. 4t). Other peculiarities in older SRA-transgenic animals included prominent ductal-alveolar retrogression along with elevated levels of granulocytes in lobulo-alveolar systems and the appearance of lipofuscin in amounts much larger than in age-matched wild-type animals (not shown).

(v) SRA promotes mitotic as well as apoptotic activities. The hyperplastic alterations observed in SRA-transgenic mammary glands pointed to increased cellular proliferation. This was confirmed by BrdU immunohistochemistry on sections of the abdominal mammary gland, which showed increased luminal epithelial cell mitosis in transgenic mice at all stages of mammary gland development. Proliferation was highest in mammary glands of virgin carriers (Fig. 5A).

At the same time, microscopic analyses also revealed abundant cell death in SRA-transgenic mammary glands. Apoptosis is irrefutably indicated by the presence of clear vacuoles and phagocytosis of dispersed clusters of apoptotic bodies by intraepithelial macrophages. While increased apoptosis was also observed in adult transgenic mammary glands, it was most prominent in the glands of younger virgin carriers, in which the numbers of apoptotic cells were about seven-fold higher than in the glands of age-matched wild-type mice (Fig. 5B). Together, these results indicated that while SRA overexpression promoted strong mitotic activities in the mammary epithelia, it also enhanced apoptosis, suggesting a role for the RNA coactivator and SRs in tissue homeostasis.

PR expression is up-regulated in SRA-transgenic mammary glands. The functions of PR in the genesis and progression of alveolar structures appear to be enhanced in SRA-transgenic glands. Because ER controls PR expression by binding to its promoter and because ER is susceptible to SRA coactivation in vitro (Fig. 6A), we hypothesized the existence of elevated PR levels in transgenic mice. Immunohistochemistry for murine PR identified significantly increased levels of PR expression in ductal epithelial cells of pubescent SRA-transgenic virgins but showed normal PR levels in transgenic multiparous mice (Fig. 6B). The increased levels of PR expression in mammary glands of younger transgenic mice correlates with the physiological function of the receptor in the mammary gland, which is controlled by ovarian estrogen and most probably is related to SRA coactivation of estrogen-induced transcription. This observation therefore indicates that ectopic expression of SRA is capable of coactivating an SR response under physiological conditions. Moreover, because PR is expressed highest in the mammary epithelial structures of the peripubertal mouse (16), the increased PR expression in SRA transgenic virgins coincides with the observation of increased cell proliferation shown in Fig. 5, suggesting a relationship between PR

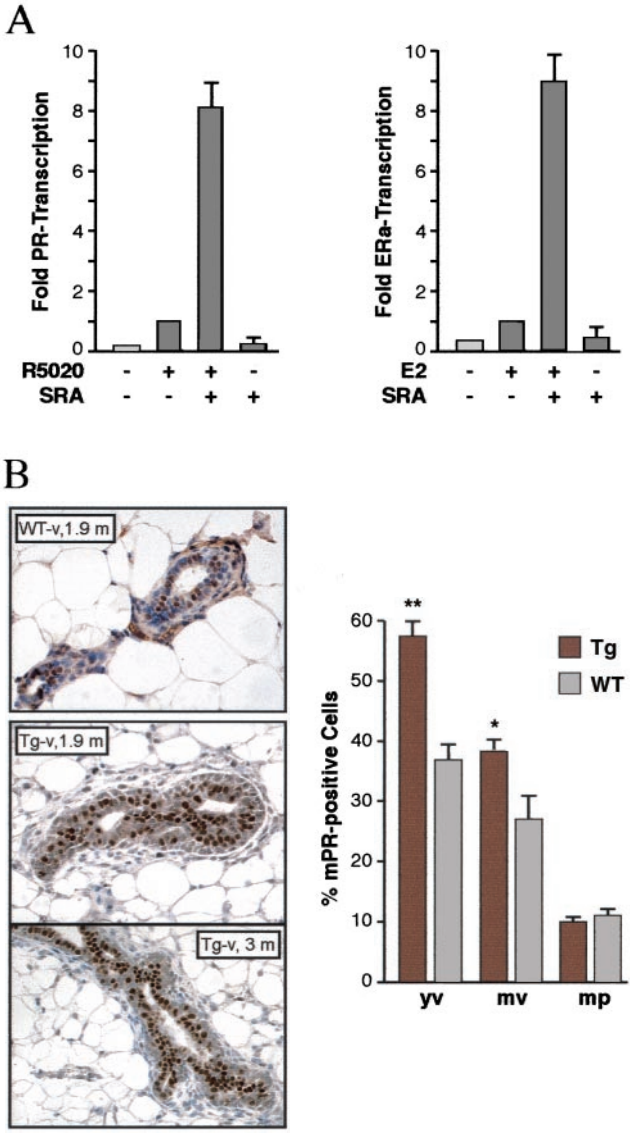

FIG. 6. Increased PR levels in glands from virgin SRA-transgenic mice. SRA-overexpressing tissues show higher response to steroid hormones. (A) Representative in vitro receptor assays illustrating ligand-dependent enhancement of receptor-mediated transcription (PR and ER, respectively) in the presence of transfected SRA. Relative transactivation of receptors was obtained by transient cotransfection of recombinant human cDNAs for PR (20 ng of pSCT-hPR [left panel]) or ER (30 ng of pSCT-ERα [right panel]), respectively, along with empty pSCT vector (−) or 1 μg of human SRA cDNA (SRA) and 2.5 μg of luciferase reporter MMTV-Luc or ERE2-Luc, respectively. R5020, 10 nM synthetic progesterone; E2, 10 nM estradiol. Relative luciferase activities are shown as the mean and standard error for three different experiments. (B) MMTV-SRA expression increased endogenous PR levels in mammary ducts of young transgenic virgins. The micrographs show immunohistochemistry for murine progesterone receptor (PR) on sections from wild-type (WT) and SRA-transgenic (Tg) virgin mammary glands. The graph illustrates number of PR-immunoreactive cells counted on sections from young virgins (yv, 3 to 6 weeks old), mature virgins (mv, 13 to 15 months old), and multiparous mice (mp, 5 to 15 months old). **, significant differences between Tg and WT mice (*t* test, $P = 0.000173$); *, by *t* test, $P = 0.0657$.

A

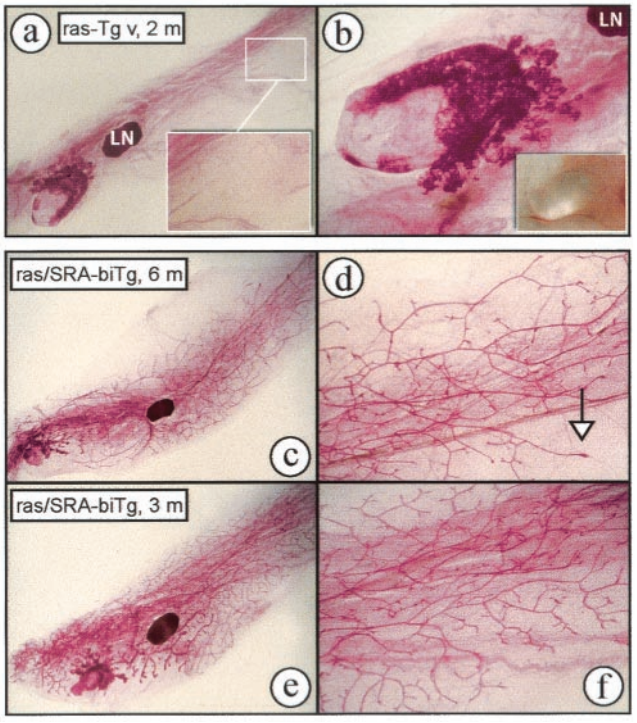

B

		ras		ras/SRA	
		#	%	#	%
I.	Necropsy; n =	27	100	18	100
	normal bga:	1	4	1	6
	mg lesions:	25	93	8	44
	sg lesions:	12	44	1	6
II.	Whole-mounts; n =	20	100	17	100
	normal bwm:	3	15	1	5
	little ductal growth:	15	75	6	35
	ductal penetration:	2	10	10	60

bga, by gross anatomy; mg, mammary gland; sg, salivary gland; bwm, by whole-mount analysis.

FIG. 7. SRA Expression obstructs ras-mediated tumorigenesis. (A) Whole-mount analyses of MMTV-ras transgenic (micrographs a and b) and ras/SRA bitransgenic (micrographs c to f) abdominal virgin mammary glands. MMTV-ras transgenic glands rarely show ductal development beyond the lymph node (LN) (micrograph a) but, instead, form focal hyperplastic structures (micrograph b), which by gross anatomy appear as blisters at an early stage of tumor development (inset in micrograph b). In contrast, ras/SRA bitransgenic mammary glands more often display ductal penetration of the entire fat pad (micrographs c and e; higher magnifications in micrographs d and f, respectively). The arrow in micrograph d points to a club-shaped terminal end bud, which serves to penetrate and populate the fat pad, indicating proliferation in service. (B) The table compares mammary gland and salivary gland tumor frequencies in MMTV-ras transgenic (ras) and MMTV-ras/SRA bitransgenic (ras/SR) mice as analyzed by necropsy (I) and whole-mounts (II). #, number of analyzed mice; %, percentage; little ductal growth, no ductal development beyond the lymph node (as illustrated in panel A); ductal penetration, normal ductal outgrowth filling the entire fad pad; other abbreviations as indicated.

transcriptional activity and cell proliferation at this stage of mammary gland development.

Mammary gland differentiation is regulated in part by prolactin and GH (27). The levels of these hormones were not found to be significantly altered in serum of SRA-transgenic mice compared to those in serum of wild-type mice (not shown). Moreover, the average weight of SRA-transgenic females was 12% lower than that of age-matched wild-type mice during the 20-month of observation (data not shown), making a contribution of GH to the formation of the described phenotypes unlikely.

SRA inhibits ras-induced tumorigenesis. The observation that preneoplastic lesions in older SRA-transgenic animals did not develop to malignancies suggested that overexpression of SRA alone was not sufficient to convert the morphological alterations to a malignant phenotype. To further test our deduction, we interbred SRA-transgenic mice with the MMTV-ras transgenic line, which produces tumors at a high rate. The lesions are palpable in MMTV-ras mice, allowing their growth rate to be easily monitored (38). To create comparable mouse models, we first interbred MMTV-ras mice from Charles River Laboratories (44) into the FVB background used for the generation of MMTV-SRA lines. MMTV-ras-transgenic FVB animals showed a variety of proliferative disturbances that were similar to the originally reported phenotypes (38). Male animals developed predominantly nonmalignant Harderian gland hyperplasia with severe exophthalmos and alopecia around the eyes secondary to glandular enlargement, along with parotid salivary gland lesions (not shown). Female animals developed spontaneous mammary tumors (adenocarcinomas and malignant lymphomas) and parotid adenocarcinomas at about 3 months of age. Mammary gland whole-mount analyses of ras-transgenic mice revealed a spatially limited ductal penetration of the fat pad with a few ductal systems forming focal hyperplastic nodules at the proximity of the primary ducts (Fig. 7A, micrographs a and b), which at an early stage of tumorigenesis were of watery consistency and resembled translucent blisters (inset in panel b).

The analysis of the ras/SRA bitransgenic animals revealed some surprising results. Of the 18 ras/SRA bitransgenic animals analyzed by necropsy, only 1 had developed salivary gland lesions and 8 (44%) showed proliferative disturbances of the mammary glands (Fig. 7B). However, the tumor rates were significantly lower than those observed in ras monogenic carriers; only 12 bitransgenic animals (44%; $n = 27$) developed salivary gland tumors and 25 (93%) formed mammary gland lesions. In addition, ras/SRA virgins showed strong ductal development with penetration of the entire fat pad (Fig. 7A, panels c to f). This morphology stands in stark contrast to the predominantly (70%; $n = 20$) ductless mammary glands of age-matched ras monogenic animals (panel a). Although repetitive parity accelerated mammary tumor formation in both ras and ras/SRA-transgenic strains, tumor onset was clearly

delayed in bitransgenic carriers, as measured by the age of the animals when critical nodule mass was first observed. While bitransgenic male mice showed delayed salivary gland perturbations, expression of transgenic SRA had no impact on harderian gland hyperplasia. When salivary gland and mammary gland tissues were investigated for ras expression, qPCR analysis showed similar levels of ras transcripts in mono- and bigenic mice, indicating that coexpression of SRA did not downregulate MMTV-ras expression (data not shown).

These results indicate that SRA function interfered with ras-induced tumor formation, which is an interesting aspect requiring further investigation. Most importantly with respect to our initial objectives, however, is the notion that overexpression of SRA in murine mammary tissue, although a factor in increased cellular proliferation and apoptosis, was not in itself sufficient to induce turmorigenesis.

Dysgenesis and hyperplasia in SRA-transgenic male mice. Because transgene expression analysis showed SRA-transcripts in the male urogenital glands (Fig. 2), we also analyzed male carriers for derangements of tissue structure and function. In wild-type male mice, the SV are large sacculated glands with similarly elongated coagulating glands attached to their concave surface. By gross analysis, transgenic SV appeared as "fist-like" structures (Fig. 8b), which varied greatly from the horn-like shape of the SV of wild-type animals (Fig. 8a). In addition, transgenic SV were mostly discolored, showed a cystic and vascular appearance, and were often encapsulated by hyperplastic prostate tissue (Fig. 8b). Compared to the intensely eosinophilic staining of the luminal portion in wild-type glands, transgenic SV showed abnormal secretion products of noneosinophilic nature (Fig. 8c). Brown hemosiderin, compact hyaline collagenous tissue, granulocytes, and macrophages (inset in Fig. 8c) within the grossly enlarged lumen of the SV suggested the existence of hemorrhage and inflammation. The dysplastic muscular surrounding of the paired gland was often found ruptured by focal inflammation, as indicated by the accumulation of lymphocytes and macrophages (Fig. 8d). The normally large acini of the simple tall columnar epithelium of the SV appeared pseudostratified and highly mucosal in distinct portions of the transgenic gland (Fig. 8e), and the presence of numerous mitotic figures and vacuolated cell structures along with apoptotic bodies in the hyperplastic epithelia indicated a high rate of cellular proliferation and concurrent cell death (Fig. 8e).

Because each coagulating gland has a fibrous capsule in common with the attached SV, SRA-transgenic coagulating glands showed aberrant morphology by adapting to the dysplastic structure of the conjoined SV. Histology, however, revealed only minor alterations in the cellular structures since simple columnar epithelia and acini with branched papillary projections of its mucosa were observed (Fig. 8f). In contrast, the dorsal lobes of the prostate of carrier animals showed portions of epithelial stratification and often contained heteromorphic cells and necrotic cellular debris in the luminal portion of the gland (Fig. 8g). The epithelial cells of the ventral lobes of SRA-transgenic prostate were mainly columnar and showed a foamy cytoplasm, which is characteristic of an actively secreting epithelium (Fig. 8h). In its entirety, the transgenic ventral prostate exhibited relatively mild histological perturbations indicated by an increased nuclear-to-cytoplasmic ratio and mild hyperplasia and disorganization with respect to the linear disposition of the luminal epithelial cells (Fig. 8h).

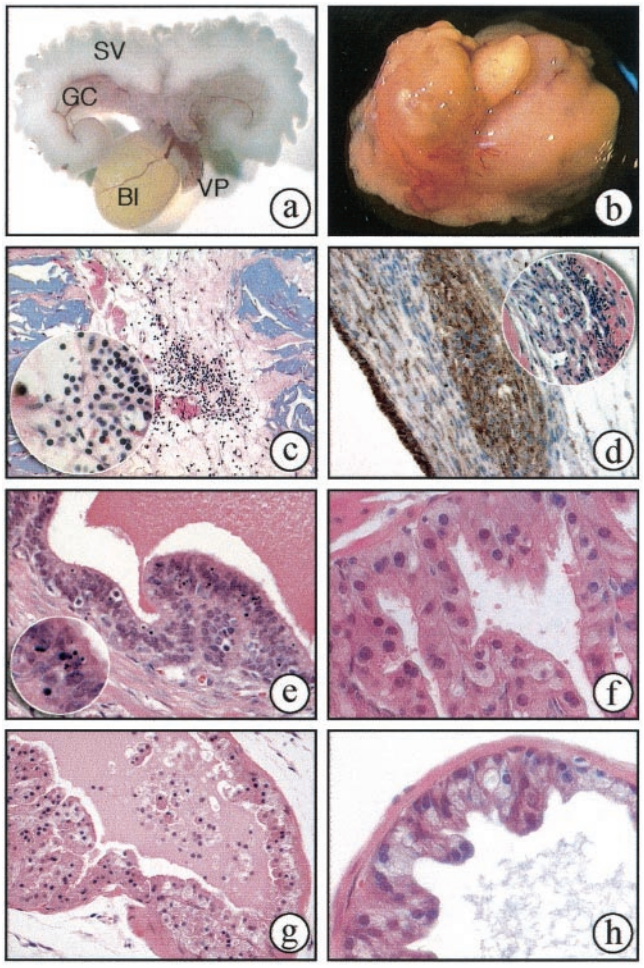

FIG. 8. Histopathology of SRA expression in the male accessory sex glands. Tissues from the male urogenital tract are shown by gross anatomy (a and b), H&E-stained histology (c to h), and Mac-3-immunohistochemistry (d). Compared to the wild type (a), SV from SRA-transgenic mice were grossly malformed (b), showed inflammation in the lumen (c) and muscular surrounding tissue (d), and displayed hyperplastic luminal epithelia with marked apoptotic activity (e). The inset in panel c shows brown hemosiderin, granulocytes, and dense-staining lymphocytes in the luminal portion of the SV; the inset in panel d shows H&E staining of the inflammation in the muscular wall of the SV, and the inset in panel e is a higher magnification of a section of the coagulating-gland epithelia showing multiple apoptotic bodies. The luminal epithelial cells of the different lobes of SRA-transgenic prostate (coagulating gland [f], dorsal prostate [g], and ventral prostate [h]) displayed various levels of hyperplasia. Bl indicates the urinary bladder.

Dysplasia of the SV and hyperplastic prostate were not observed in prepubescent SRA mice, which indicated that SRA functions in response to the elevated levels of systemic hormones and growth signals in these organs during pubescence. Because AR is a target for SRA coactivation in tissue culture cells (18) and because testosterone levels surge during this developmental stage, we concluded that SRA plays a role in the testosterone-controlled formation of the male accessory sex glands. The ectopic expression of SRA, however, did not

significantly change androgen receptor levels in prostate and testis tissues as assayed by Western blotting (not shown).

Germinal aplasia in the SRA-transgenic testis. We also examined the testes, epididymi and vas deferens for SRA-related growth perturbations. While the cauda and caput epididymi and vas deferens appeared normal in our analyses, histology of SRA-transgenic testes revealed severe germinal aplasia. In these testes, up to 50% of seminiferous tubules appeared vacuolated or were devoid of spermatogenic cells (Fig. 9A, micrograph b). Sloughing of germ cells into the lumen indicated that spermatogenesis was not completely absent in these tubules (micrograph c), while intraluminal eosinophilic secretions, hemosiderin, and infiltrates of macrophages strongly indicated a disruption of the luminal seminiferous epithelium formed by the Sertoli cells (micrograph d). A breakdown of the blood-testis barrier formed by the Sertoli-Sertoli junctional complex was also suggested by the identification of mononuclear phagocytes in the luminal compartment of the tubules, as shown by immunohistochemistry for Mac-3 antigen (micrograph d). The degeneration of the seminiferous tubules resulted in a reduced testis size relative to body weight in adult SRA-transgenic mice (180 to 400 days old; 3.17 mg/g for wild-type mice and 2.74 mg/g for transgenic mice; $P = 0.00087$) but not in adolescent mice (40 to 50 days old; 3.46 mg/g for wild-type mice and 3.68 mg/g for transgenic mice; $P = 0.0742$). Histology also showed abundant hypertrophic intrastitial Leydig cells with abundant cytoplasmic vacuoles in SRA-transgenic testes (Fig. 9B). Because Leydig cells secrete testosterone, we assumed that the vacuoles in the Leydig cells represented extracted lipids. Our hypothesis was supported by radioimmunoassays, which revealed significantly elevated serum testosterone levels in SRA-transgenic males (Fig. 9B). We concluded that the relatively high testosterone levels in carrier animals were most probably the consequence of efflux of the hormone into the intratesticular microvascular system due to the disrupted seminiferous epithelium.

To summarize, MMTV-controlled expression of human SRA resulted in various effects on murine organ development but was, in itself, not sufficient to induce turmorigenesis. Although abundant SRA in general showed strong promoting activities on proliferation and differentiation, it also enhanced apoptosis. Little to no cellular pleomorphism was observed, and preneoplastic lesions were cleared by focal degenerative transformations.

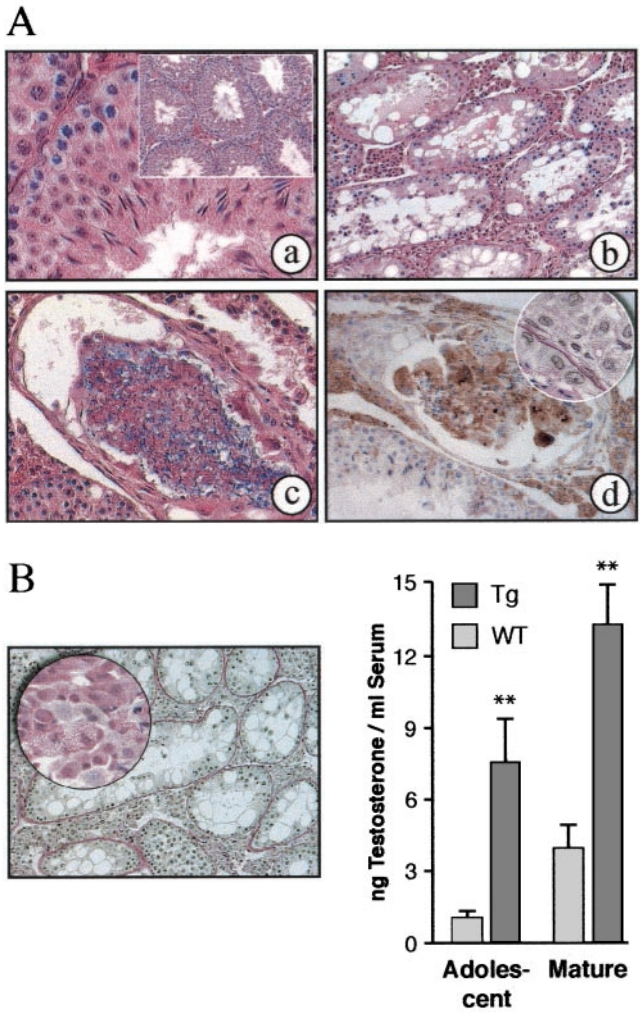

FIG. 9. Germinal aplasia and elevated testosterone levels in SRA mice. (A) SRA-transgenic testes displayed dysgenesis of the seminifeous tubules. H&E histology (micrographs a to d), PAS staining (inset in micrograph d), and Mac-3 immunohistochemistry (micrograph d) of wild-type (micrograph a) and SRA-transgenic (micrographs b to d) testes. The seminiferous tubules appear vacuolated (micrograph b), show sloughing of germ cell elements into the lumen (micrograph c), and have greatly disrupted luminal seminiferous epithelia (inset in micrograph d). Intraluminal eosinophilic secretions, hemosiderin, and infiltrates of lymphocytes and monocytes (micrograph d) indicate a breakdown of the blood-testis barrier formed by the Sertoli-Sertoli junctional complex. (B) Leydig cell hyperplasia and elevated serum testosterone levels. Histology of periodic acid-Schiff-stained sections from an SRA-transgenic testis illustrate numerous intrastitial Leydig cells with copious and vacuolated cytoplasm (inset, H&E staining). Critically elevated serum testosterone levels in adolescent and mature SRA-transgenic males were detected by radioimmunoassays (chart). **, Significant differences between transgenic (Tg) and wild-type (WT) mice; 6 weeks: $n_{WT} = 14$, $n_{Tg} = 12$ (t test, $P = 0.00035$); 6 months: $n_{WT} = 3$, $n_{Tg} = 6$ (t test, $P = 0.00009$).

DISCUSSION

The strong up-regulation of SRA in various tumors of the human breast, uterus, and ovary, together with its relatively low expression in normal tissues, suggests a role for the RNA activator as a biological marker of steroid-dependent tumors. While additional studies and in situ analysis are necessary to validate SRA as predictive diagnostic marker, its expression profile in breast tissues is in agreement with previous findings (26). In addition, because SRA was expressed at high levels regardless of tumor type, a role in early turmorigenesis is implicated. To assess the pathogenic potential of SRA in vivo, an MMTV-SRA-transgenic mouse model was generated and analyzed. All SRA-transgenic lines produced tumor-free animals that exhibited a life span comparable to that of wild-type animals, indicating that overexpression of SRA is not in itself sufficient to induce tumors.

Still, SRA-transgenic mice displayed a plethora of phenotypes, which have to be viewed in relation to the various functions of SRs expressed in the target tissues. Few SR-transgenic models exist, and the physiological roles of SRs have been

based largely on the characterization of mouse models genetically ablated for a specific receptor function. Because of the intricate circuitry of steroid actions, coordinated receptor function is often disrupted in these animals. In this respect, MMTV-SRA-transgenic mice display overall elevated SR activities and therefore provide a model that accounts for coordinated functions of the receptors and their isoforms.

The proliferative phenotypes observed in mammary glands of SRA-transgenic mice resemble the physiological changes reported for PR-A-transgenic mice (37). Although the levels of PR isoforms are altered in these mice, their mammary gland development primarily reflects increased responsiveness to progestins. By comparative analysis, the morphological changes observed in SRA-transgenic mammary glands may be partially attributed to SRA-potentiated PR activity. While SRA may affect mammary gland development through PR transactivation, PR expression itself is also modulated by ovarian estrogen, whose levels in serum are elevated during puberty and pregnancy. Proper individual mechanistic roles for progesterone and estrogen in vivo have yet to be established, but the supposition from the targeted deletion of PR (22) and the ERα knockout (1, 9) models emphasizes the specific role of estrogen rather than progesterone in mammary gland ductal elongation during puberty (40). At this particular stage of mammary development, SRA-transgenic mammary glands showed significantly elevated levels of PR expression (Fig. 6B). Because this expression profile subsided as the virgins matured and because it correlates with ovarian estrogen signaling in mammary ductal outgrowth, our results suggested the presence of SRA-enhanced ER transactivation of the *PR* gene and provided us with the first distinctive evidence for an SRA function in vivo.

PR, as both a target for SRA function and a key molecule to transmit the actions of endocrine mammogens, is expressed at the highest level in the mammary epithelial structures of the peripubertal (5-weak-old) mouse (16). The expression profile of PR coincides with the appearance of ductal epithelial proliferation and multilocular fat in SRA-transgenic mice at this stage of mammary gland development. Mammary fat tissue plays a crucial role in epithelial growth and lobulo-alveolar morphogenesis of the mammary parenchyma (11, 32, 33). While it was long assumed that the mammary fat was composed exclusively of energy-storing white adipose tissue, energy-dissipating brown adipose tissue (BAT) (17) has recently been reported to occupy temporal and spatial compartments in the mammary gland stroma (13, 25). While promoting concurrent PR functions, SRA overexpression also enhanced the appearance of BAT at this time in mammary gland development, suggesting that the dedifferentiation of adipose tissue is related to the paracrine signaling (3) that is part of the progesterone-induced proliferative signals. This hypothesis is supported by the enhanced complexity of mammary ductal branching observed in a transgenic mouse model depleted of BAT. In this model, brown fat, in contrast to white adipose tissue, negatively regulated the differentiation of transplanted mammary epithelial cells during peripubertal ductal outgrowth (13). This observation suggests that the abnormal branching morphology observed in SRA-transgenic virgins may be the consequence of the temporal exposure of the young ductal system to excessive BAT. In addition, while the developmental and environmental stimuli responsible for adaptive thermogenesis in the mammary gland are still theoretical (13, 25), the dramatic temporal increase in BAT in mammary glands of young SRA-transgenic mice may suggest a paracrine function for the RNA activator in this process.

Under pathological conditions, apoptosis results in the regression of neoplastic tissue, as well as substantial cell loss and retardation of cancer growth (2). In SRA-transgenic mice, augmented apoptosis was observed to counteract strong mitotic activities and, assisted by inflammatory responses, to clear metaplastic tissues and ductal structures. The mechanism by which SRA mediates the balance between proliferation and apoptosis is not known. However, it is important to reiterate the plasticity of the mammary gland (27, 43). This allows for speculation about an intrinsic attempt by the mammary gland to ensure the specification and spatial organization of ductal and alveolar structures. PR plays an important role in this process (16, 36), which is tested and reestablished by recurring parturition. The observation that early first pregnancy reduces the risk of breast cancer supports this notion (41). Early parity-induced protection against mammary cancer involves p53-mediated signaling (39). Investigation of SRA-associated molecules resulted in the identification of a protein that specifically binds to RNA substructure STR1 of SRA (19; A. Redfem, D. Beveridge, R. B. Lanz, L. Stuart, B. O'Malley, and P. Leedman, Proc. Endocr. Soc. 84th Annu. Meet., abstr. OR46-6, 2002). This protein was functionally linked to the p53 and NF-κB pathways and, as such, provides a molecular link between SRA function and apoptosis, inflammation, and parity-induced tumor protection (39). Still, further experiments are necessary to delineate the specific roles of SRA and SR in mammary gland tissue homeostasis.

The significantly lower tumor rates observed in ras/SRA-bitransgenic mice provided more evidence of the antitumorigenic potential of SRA, a presumptive function of the RNA coactivator that will have to be confirmed by using other bitransgenic mouse models. In contrast to the SRA-transgenic models, no phenotypic abnormalities have been observed by the targeted deletion of the *SRA* gene (unpublished result), suggesting that a functionally redundant molecule may compensate for the phenotype. SRA overexpression, however, triggered proliferation, inflammation, and apoptosis in estrogen, progesterone, and testosterone-sensitive tissues of male and female mice, suggesting a physiological role for the RNA activator in the establishment of tissue homeostasis in steroidal tissues. Our results raise the possibility that in contrast to our initial conclusions, the up-regulation of SRA in many human tumors of steroid-dependent tissue may reflect a cellular effort to antagonize excessive proliferation. Additional studies will eventually elucidate the mechanisms involved. It is possible that tumor progression is controlled by the specific composition of ribonucleoprotein complexes containing SRA, whose expression level determines whether transcriptional coactivators or corepressors are incorporated. This model is consistent with to the reported role of SRA in attenuation of SR transactivation in conjunction with SHARP (35). Even so, our analyses of SRA mouse models suggest that the promotion of proliferating functions used to achieve established tissue structures occurs in conjunction with mechanisms to prevent tumor formation.

ACKNOWLEDGMENTS

We thank J. Lydon, D. Medina, and J. Rosen for helpful discussion; E. Hayes and F. Moormehei for technical assistance; W. J. Muller for the Mmtv-Sv40-Bssk plasmid; and P. Ismail and K. Schillinger for help with PR-immunohistochemistry and the manuscript; respectively.

This work was supported by grants from the Texas Higher Education Advanced Technology Program (ATP 004949-0154-1999), from The CONCERN Foundation, SPORE P50CA58183 Breast Cancer, and the Edward Mallinckrodt Jr. Foundation to R.B.L. and by an HD-NIH grant to B.W.O.

REFERENCES

1. **Bocchinfuso, W. P., and K. S. Korach.** 1997. Mammary gland development and tumorigenesis in estrogen receptor knockout mice. J. Mammary Gland Biol. Neoplasia **2:**323–334.
2. **Bonnette, S. G., F. S. Kittrell, L. C. Stephens, R. E. Meyn, and D. Medina.** 1999. Interactions of apoptosis, proliferation and host age in the regression of the mouse mammary preneoplasia, TM3, carrying an unusual mutation in p53. Carcinogenesis **20:**1715–1720.
3. **Brisken, C., S. Park, T. Vass, J. P. Lydon, B. W. O'Malley, and R. A. Weinberg.** 1998. A paracrine role for the epithelial progesterone receptor in mammary gland development. Proc. Natl. Acad. Sci. USA **95:**5076–5081.
4. **Cardiff, R. D.** 2001. Validity of mouse mammary tumour models for human breast cancer: comparative pathology. Microsc. Res. Tech. **52:**224–230.
5. **Choi, Y. W., D. Henrard, I. Lee, and S. R. Ross.** 1987. The mouse mammary tumor virus long terminal repeat directs expression in epithelial and lymphoid cells of different tissues in transgenic mice. J. Virol. **61:**3013–3019.
6. **Chomczynski, P., and N. Sacchi.** 1987. Single-step method of RNA isolation by acid guanidinium thiocyanate-phenol-chloroform extraction. Anal. Biochem. **162:**156–159.
7. **Chua, S. S., Z. Q. Ma, L. Gong, S. H. Lin, F. J. DeMayo, and S. Y. Tsai.** 2002. Ectopic expression of FGF-3 results in abnormal prostate and Wolffian duct development. Oncogene **21:**1899–1908.
8. **Church, G. M., and W. Gilbert.** 1984. Genomic sequencing. Proc. Natl. Acad. Sci. USA **81:**1991–1995.
9. **Couse, J. F., and K. S. Korach.** 1999. Estrogen receptor null mice: what have we learned and where will they lead us? Endocr. Rev. **20:**358–417.
10. **Cox, K. H., D. V. DeLeon, L. M. Angerer, and R. C. Angerer.** 1984. Detection of mRNAs in sea urchin embryos by in situ hybridization using asymmetric RNA probes. Dev. Biol. **101:**485–502.
11. **DeOrne, K. B., L. J. Faulkin, H. A. Bern, and P. B. Blair.** 1959. Development of mammary tumors from hyperplastic alveolar nodules transplanted into gland-free mammary fat pads of females C3H mice. Cancer Res. **19:**515.
12. **Donehower, L. A., A. L. Huang, and G. L. Hager.** 1981. Regulatory and coding potential of the mouse mammary tumor virus long terminal redundancy. J. Virol. **37:**226–238.
13. **Gouon-Evans, V., and J. W. Pollard.** 2002. Unexpected deposition of brown fat in mammary gland during postnatal development. Mol. Endocrinol. **16:**2618–2627.
14. **Huang, A. L., M. C. Ostrowski, D. Berard, and G. L. Hager.** 1981. Glucocorticoid regulation of the Ha-MuSV p21 gene conferred by sequences from mouse mammary tumor virus. Cell **27:**245–255.
15. **Hutchinson, J. N., and W. J. Muller.** 2000. Transgenic mouse models of human breast cancer. Oncogene **19:**6130–6137.
16. **Ismail, P. M., J. Li, F. J. DeMayo, B. W. O'Malley, and J. P. Lydon.** 2002. A novel LacZ reporter mouse reveals complex regulation of the progesterone receptor promoter during mammary gland development. Mol. Endocrinol. **16:**2475–2489.
17. **Klaus, S.** 1997. Functional differentiation of white and brown adipocytes. Bioessays **19:**215–223.
18. **Lanz, R. B., N. J. McKenna, S. A. Onate, U. Albrecht, J. Wong, S. Y. Tsai, M. J. Tsai, and B. W. O'Malley.** 1999. A steroid receptor coactivator, SRA, functions as an RNA and is present in an SRC-1 complex. Cell **97:**17–27.
19. **Lanz, R. B., B. Razani, A. D. Goldberg, and B. W. O'Malley.** 2002. Distinct RNA motifs are important for coactivation of steroid hormone receptors by steroid receptor RNA activator (SRA). Proc. Natl. Acad. Sci. USA **99:**16081–16086.
20. **Leygue, E., H. Dotzlaw, P. H. Watson, and L. C. Murphy.** 1999. Expression of the steroid receptor RNA activator in human breast tumors. Cancer Res. **59:**4190–4193.
21. **Li, Y., W. P. Hively, and H. E. Varmus.** 2000. Use of MMTV-Wnt-1 transgenic mice for studying the genetic basis of breast cancer. Oncogene **19:**1002–1009.
22. **Lydon, J. P., F. J. DeMayo, C. R. Funk, S. K. Mani, A. R. Hughes, C. A. Montgomery, Jr., G. Shyamala, O. M. Conneely, and B. W. O'Malley.** 1995. Mice lacking progesterone receptor exhibit pleiotropic reproductive abnormalities. Genes Dev. **9:**2266–2278.
23. **Mangelsdorf, D. J., C. Thummel, M. Beato, P. Herrlich, G. Schutz, K. Umesono, B. Blumberg, P. Kastner, M. Mark, P. Chambon, et al.** 1995. The nuclear receptor superfamily: the second decade. Cell **83:**835–839.
24. **Marquis, S. T., J. V. Rajan, A. Wynshaw-Boris, J. Xu, G. Y. Yin, K. J. Abel, B. L. Weber, and L. A. Chodosh.** 1995. The developmental pattern of Brca1 expression implies a role in differentiation of the breast and other tissues. Nat. Genet. **11:**17–26.
25. **Master, S. R., J. L. Hartman, C. M. D'Cruz, S. E. Moody, E. A. Keiper, S. I. Ha, J. D. Cox, G. K. Belka, and L. A. Chodosh.** 2002. Functional microarray analysis of mammary organogenesis reveals a developmental role in adaptive thermogenesis. Mol. Endocrinol. **16:**1185–1203.
26. **Murphy, L. C., S. L. Simon, A. Parkes, E. Leygue, H. Dotzlaw, L. Snell, S. Troup, A. Adeyinka, and P. H. Watson.** 2000. Altered expression of estrogen receptor coregulators during human breast tumorigenesis. Cancer Res. **60:**6266–6271.
27. **Neville, M. C., and C. W. Daniel.** 1987. The mammary gland: development, regulation, and function. Plenum Press, New York, N.Y.
28. **Norris, J. D., D. Fan, A. Sherk, and D. P. McDonnell.** 2002. A negative coregulator for the human ER. Mol. Endocrinol. **16:**459–468.
29. **Pattengale, P. K., T. A. Stewart, A. Leder, E. Sinn, W. Muller, I. Tepler, E. Schmidt, and P. Leder.** 1989. Animal models of human disease. Pathology and molecular biology of spontaneous neoplasms occurring in transgenic mice carrying and expressing activated cellular oncogenes. Am. J. Pathol. **135:**39–61.
30. **Prins, G. S., and L. Birch.** 1995. The developmental pattern of androgen receptor expression in rat prostate lobes is altered after neonatal exposure to estrogen. Endocrinology **136:**1303–1314.
31. **Said, T. K., O. M. Conneely, D. Medina, B. W. O'Malley, and J. P. Lydon.** 1997. Progesterone, in addition to estrogen, induces cyclin D1 expression in the murine mammary epithelial cell, in vivo. Endocrinology **138:**3933–3939.
32. **Sakakura, T., Y. Nishizuka, and C. J. Dawe.** 1976. Mesenchyme-dependent morphogenesis and epithelium-specific cytodifferentiation in mouse mammary gland. Science **194:**1439–1441.
33. **Sakakura, T., Y. Sakagami, and Y. Nishizuka.** 1982. Dual origin of mesenchymal tissues participating in mouse mammary gland embryogenesis. Dev. Biol. **91:**202–207.
34. **Seagroves, T. N., J. P. Lydon, R. C. Hovey, B. K. Vonderhaar, and J. M. Rosen.** 2000. C/EBPbeta (CCAAT/enhancer binding protein) controls cell fate determination during mammary gland development. Mol. Endocrinol. **14:**359–368.
35. **Shi, Y., M. Downes, W. Xie, H. Y. Kao, P. Ordentlich, C. C. Tsai, M. Hon, and R. M. Evans.** 2001. Sharp an inducible cofactor that integrates nuclear receptor repression and activation. Genes Dev. **15:**1140–1151.
36. **Shyamala, G., X. Yang, R. D. Cardiff, and E. Dale.** 2000. Impact of progesterone receptor on cell-fate decisions during mammary gland development. Proc. Natl. Acad. Sci. USA **97:**3044–3049.
37. **Shyamala, G., X. Yang, G. Silberstein, M. H. Barcellos-Hoff, and E. Dale.** 1998. Transgenic mice carrying an imbalance in the native ratio of A to B forms of progesterone receptor exhibit developmental abnormalities in mammary glands. Proc. Natl. Acad. Sci. USA **95:**696–701.
38. **Sinn, E., W. Muller, P. Pattengale, I. Tepler, R. Wallace, and P. Leder.** 1987. Coexpression of MMTV/v-Ha-ras and MMTV/c-myc genes in transgenic mice: synergistic action of oncogenes in vivo. Cell **49:**465–475.
39. **Sivaraman, L., S. G. Hilsenbeck, L. Zhong, J. Gay, O. M. Conneely, D. Medina, and B. W. O'Malley.** 2001. Early exposure of the rat mammary gland to estrogen and progesterone blocks co-localization of estrogen receptor expression and proliferation. J. Endocrinol. **171:**75–83.
40. **Soyal, S., P. M. Ismail, J. Li, B. Mulac-Jericevic, O. M. Conneely, and J. P. Lydon.** 2002. Progesterone's role in mammary gland development and tumorigenesis as disclosed by experimental mouse genetics. Breast Cancer Res. **4:**191–196.
41. **Spicer, D. V., E. A. Krecker, and M. C. Pike.** 1995. The endocrine prevention of breast cancer. Cancer Investig. **13:**495–504.
42. **Stewart, T. A., P. K. Pattengale, and P. Leder.** 1984. Spontaneous mammary adenocarcinomas in transgenic mice that carry and express MTV/myc fusion genes. Cell **38:**627–637.
43. **Strange, R., F. Li, S. Saurer, A. Burkhardt, and R. R. Friis.** 1992. Apoptotic cell death and tissue remodelling during mouse mammary gland involution. Development **115:**49–58.
44. **Taketo, M., A. C. Schroeder, L. E. Mobraaten, K. B. Gunning, G. Hanten, R. R. Fox, T. H. Roderick, C. L. Stewart, F. Lilly, C. T. Hansen, et al.** 1991. FVB/N: an inbred mouse strain preferable for transgenic analyses. Proc. Natl. Acad. Sci. USA **88:**2065–2069.
45. **Tsai, M. J., and B. W. O'Malley.** 1994. Molecular mechanisms of action of steroid/thyroid receptor superfamily members. Annu. Rev. Biochem. **63:**451–486.
46. **Watanabe, M., J. Yanagisawa, H. Kitagawa, K. Takeyama, S. Ogawa, Y. Arao, M. Suzawa, Y. Kobayashi, T. Yano, H. Yoshikawa, Y. Masuhiro, and S. Kato.** 2001. A subfamily of RNA-binding DEAD-box proteins acts as an estrogen receptor alpha coactivator through the N-terminal activation domain (AF-1) with an RNA coactivator, SRA. EMBO J. **20:**1341–1352.